

# Superhumps in the cataclysmic variable BG Tri

S. Y. Stefanov,<sup>1,2</sup> G. Latev,<sup>1,3</sup> S. Boeva,<sup>1</sup> M. Moyseev<sup>1,2</sup>

<sup>1</sup>*Institute of Astronomy and National Astronomical Observatory, Bulgarian Academy of Sciences, Tsarigradsko Shose 72, BG-1784 Sofia, Bulgaria*

<sup>2</sup>*Department of Astronomy, Sofia University "St. Kliment Ohridski", James Bourchier 5, BG-1164 Sofia, Bulgaria*

<sup>3</sup>*Astronomical Association Sofia, Tsar Asen 49, BG-1463 Sofia, Bulgaria*

Accepted XXX. Received YYY; in original form ZZZ

## ABSTRACT

We present a detailed photometric study of the bright cataclysmic variable BG Tri using ground-based observations mainly from Rozhen Observatory, ASAS-SN, TESS, and WASP sky surveys. We report the discovery of a negative superhump with  $P_{-sh} = 0.1515(2)$  days and a co-existing superorbital variation with  $P = 3.94(53)$  days in data from 2019 and 2020. A positive superhump with  $P_{+sh} = 0.1727(14)$  days is also discovered in data from 2006. The obtained negative superhump deficit  $\varepsilon_- = 0.044(1)$  and the positive superhump excess  $\varepsilon_+ = 0.090(9)$  give us an independent photometric evaluation of the mass ratio ( $q$ ) of the system, which we find to be  $q_- = 0.37(2)$  and  $q_+ = 0.40(5)$  respectively. We also present a study of the quasi-periodic oscillations (QPOs) and stochastic variability (flickering) in BG Tri. The light curves show a rich mixture of simultaneously overlapping quasi-periods ranging from 5 to 25 minutes. The multi-color ( $UBVRI$ ) photometric observations from Rozhen Observatory reveal the typical increase of the flickering amplitudes to the shorter wavelengths. The recently introduced  $A_{60}$  amplitude of the flickering light source in all studied photometric bands is systematically lower when the negative superhump is gone in season 2021.

**Key words:** stars: activity – (stars:) binaries: close – (stars:) novae, cataclysmic variables – stars: individual: BG Tri

## 1 INTRODUCTION

Cataclysmic variables (CVs) are close binary systems consisting of a Roche-lobe filling secondary, orbiting an accreting white dwarf primary. The secondaries in CVs are usually a low mass main-sequence star (most often a red dwarf, losing matter through the inner Lagrange point ( $L_1$ )). The transferred matter forms an accretion disc around the white dwarf, which is the primary source of the system's luminosity (Warner 2003; Hellier 2001).

Due to the Roche lobe geometry, the secondary star has a teardrop shape with the apex pointing towards the primary. This, in combination with the orbital motion of the system, results in the so-called ellipsoidal modulations (fainter for low-inclination binaries). Detecting these is a direct way to determine the orbital period of the cataclysmic variables (Hellier 2001). Along with the orbital periodicity, some CVs display periodic changes in brightness with periods close to the orbital period called superhumps. This phenomenon is commonly seen and comprehensively studied in SU UMa stars - subclass of dwarf novae CVs (e.g., Hirose & Osaki 1990; Kato et al. 2009, 2017). It is believed that a precessing accretion disc can cause such photometric behaviour. Superhumps can either be positive (apsidal - a few percent longer than the orbital period ( $P_{orb}$ )), or negative (nodal) - a few percent shorter. Superhumps can also appear in other sub-classes of CVs. Reports for 15 nova-likes (NLs - a subclass of CVs in the permanently high photometric state) with positive and 11 NLs with negative superhumps can be found in the literature (e.g., Pavlenko et al. 2020; Ritter & Kolb 2005; Castro Segura et al. 2021; Hkiewicz et al. 2021). The existence of both periodicities has been observed in some systems - TT Ari (Belova et al. 2013; Kraicheva et al. 1999), AQ Men (Hkiewicz et al. 2021), and LS Cam (Rawat

et al. 2022; Stefanov 2021). Positive superhumps are believed to appear when tidal stresses from the secondary affect the disc and cause apsidal precession in the prograde direction (e.g., Lubow 1991). Negative superhumps can be explained by a retrograde nodal precession of a tilted accretion disc. The stream impacts the face of the disc and the retrograde precession causes periods shorter than  $P_{orb}$  (e.g., Wood et al. 2009; Montgomery 2009).

BG Tri was discovered and classified as a cataclysmic variable by Khruslov (2008). Although the system is a bright CV (11.9 mag in  $V$ ), it is poorly studied. Other mentions in the literature include a cross-association with X-ray sources by Haakonsen & Rutledge (2009). In Makarov (2017), BG Tri is shown to have significant excess in near UV. In 2018 the star dropped in brightness by 2.5 mag in  $V$  and was classified as a VY Scl subclass by Kato (2018). The variables in this subclass of nova-like CVs are predominately in high photometric state except for rare brightness drops up to 6 magnitudes lasting from a few weeks to a few years.

The first comprehensive study of BG Tri was published by Hernández et al. (2021), where the system is shown to have the spectroscopic characteristics of RW Sex-type and similar nova-like variables. These variables have high mass transfer rates and bright accretion discs. The authors estimate the inclination angle as  $i = 25(5)^\circ$ , the mass of the primary  $0.8M_\odot$ , the mass of the secondary  $0.3M_\odot$ , and the binary separation -  $1.23R_\odot$ . The orbital period is measured to be 3.8028(24) hours.

Here we present photometric data of BG Tri from ground-based observations and sky surveys. We report the detection of superhump variability for the first time in BG Tri. In addition, we analyse the long

**Table 1.** Journal of observations

| Date       | Length (hr) | Filters      | Telescope            |
|------------|-------------|--------------|----------------------|
| 2020/08/11 | 2.34        | <i>UBVRI</i> | 25 cm Newton         |
| 2020/08/17 | 3.72        | <i>BV</i>    | 25 cm Newton         |
| 2020/08/22 | 1.56        | <i>UBVRI</i> | 50/70 cm Schmidt     |
| 2020/09/22 | 4.99        | <i>UBVRI</i> | 50/70 cm Schmidt     |
| 2020/09/23 | 5.88        | <i>UBVRI</i> | 50/70 cm Schmidt     |
| 2020/09/24 | 3.14        | <i>UBVRI</i> | 50/70 cm Schmidt     |
| 2020/09/25 | 8.34        | <i>BV</i>    | 50/70 cm Schmidt     |
| 2020/10/13 | 1.84        | <i>UV</i>    | 2.0 m RCC            |
| 2020/10/14 | 4.48        | <i>UV</i>    | 2.0 m RCC            |
| 2020/10/14 | 0.74        | <i>BVRI</i>  | 50/70 cm Schmidt     |
| 2020/12/21 | 0.53        | <i>UV</i>    | 2.0 m RCC            |
| 2021/01/18 | 3.61        | <i>UV</i>    | 2.0 m RCC            |
| 2021/01/18 | 2.41        | <i>BRI</i>   | 50/70 cm Schmidt     |
| 2021/01/20 | 4.25        | <i>UBVRI</i> | 50/70 cm Schmidt     |
| 2021/10/04 | 1.80        | <i>UBVRI</i> | 50/70 cm Schmidt     |
| 2021/10/06 | 1.50        | <i>UBVRI</i> | 50/70 cm Schmidt     |
| 2021/10/30 | 4.11        | <i>V</i>     | 43.2 cm Dall-Kirkham |
| 2021/11/06 | 8.21        | <i>V</i>     | 2.0 m RCC            |
| 2021/11/07 | 2.45        | <i>V</i>     | 2.0 m RCC            |
| 2021/11/07 | 2.82        | <i>UBVRI</i> | 50/70 cm Schmidt     |
| 2021/11/08 | 2.82        | <i>UBVRI</i> | 50/70 cm Schmidt     |

and short-term variability - superorbital periodicity, quasi-periodic oscillations (QPOs), and flickering.

## 2 OBSERVATIONS, DATA REDUCTION, AND PHOTOMETRY

Our first photometric data were gathered during the 2020 summer school of astronomy and astrophysics "Beli Brezi" with a 25 cm Newton telescope ( $FOV = 51' \times 39'$ ) equipped with a QHY9 CCD ( $5.4\mu\text{m}$   $3358 \times 2536$  pix) camera and standard Johnson-Cousins *UBVRI* filters. Later, in the period from August 2020 to November 2021 several observations in the *UBVRI* bands were carried out at Rozhen National Astronomical Observatory (NAO) in Bulgaria on the 50/70 cm Schmidt telescope ( $FOV = 73' \times 73'$ ) equipped with FLI PL16803 CCD ( $9\mu\text{m}$  square  $4096 \times 4096$  pix) and the 2.0 m RCC telescope ( $FOV = 10' \times 10'$ ) with two-channel focal reducer FoReRo2 (Jockers et al. 2000), attached to the Ritchey–Chrétien focus and equipped with two ANDOR iKON-L CCDs ( $13.5\mu\text{m}$  square  $2048 \times 2048$  pix). One additional light curve was obtained on the PWI SDK 17" (43.2 cm corrected Dall-Kirkham) telescope ( $FOV = 43' \times 43'$ ) at Andromeda Observatory - equipped with Alta Apogee U16M CCD ( $9\mu\text{m}$  square  $4096 \times 4096$  pix). A total of 70 hours of simultaneous and quasi-simultaneous observations in two to five bands were acquired. The majority of observing runs were longer than two hours. A journal of the observations is presented in Table 1. All photometric data were dark or bias subtracted and flat-fielded. To extract the stellar magnitudes, standard aperture photometry was applied using two to five comparison stars depending on the angular size of the frame. The gathered light curves are shown in Figure 1.

In addition to our photometry, data from several sky surveys was also analysed - The All-Sky Automated Survey for Supernovae (ASAS-SN) (Shappee et al. 2014; Kochanek et al. 2017), Catalina Real-Time Transient Survey (CRTS) (Drake et al. 2009), Wide Angle Search for Planets (WASP) (Butters et al. 2010), and the Northern Sky Variability Survey (NSVS) (Woźniak et al. 2004). A combined light curve is shown in Figure 2.

Photometry of BG Tri with 1426s cadence from sector 17 of the Transiting Exoplanet Survey Satellite TESS (Ricker et al. 2015) was

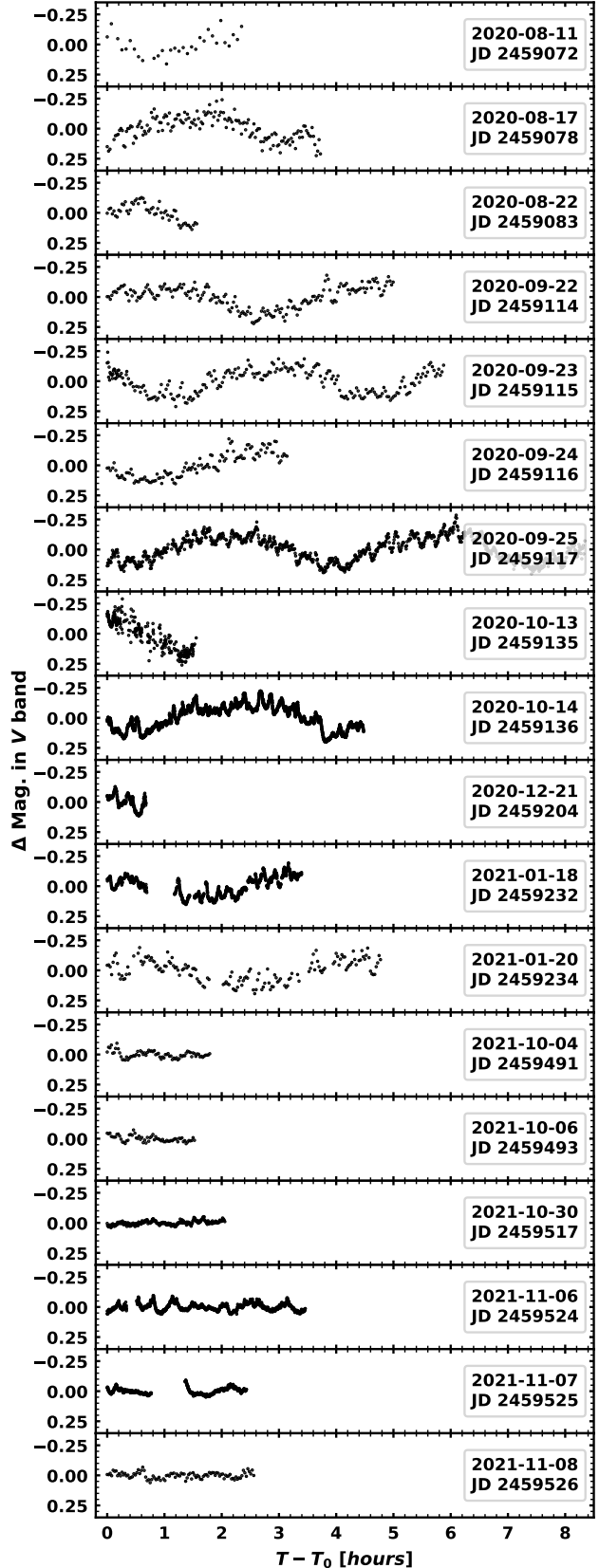


**Figure 1.** All light curves in V band listed in Table 1. The calendar date and Julian date of each observation are in the right side of the panels. The light curves are shown in relative magnitude (average subtracted) for clarity.

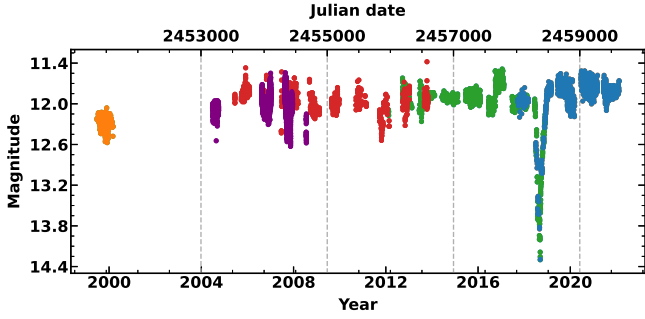


**Figure 2.** The long term behaviour of BG Tri in 1999-2021. This light curve is built with data from several sky surveys, but the magnitudes are not transformed to a single band. The color key is as follows - NSVS magnitudes (orange), WASP magnitudes (purple), CRTS magnitudes (red), ASAS-SN V band magnitudes (green) and ASAS-SN g band magnitudes (blue).

acquired using the Python package "Lightkurve" (Lightkurve Collaboration et al. 2018) and its dependencies (Brasseur et al. 2019; Ginsburg et al. 2019; Astropy Collaboration et al. 2013, 2018). Custom aperture photometry of the TESS data was performed using this package. The resulting light curve is shown in the top left panel of Figure 4.

### 3 DATA ANALYSIS, RESULTS, AND DISCUSSION

Sky survey data span 22 years. The mean magnitude of the star in the high state is  $\sim 11.9$  mag in V band and varies with an amplitude of  $\sim 0.5$  mag. Only one observed low state was detected in 2018-2019. The decline and rise rates are described in detail in Hernández et al. (2021). The drop in brightness with 2.5 mag is typical for VY Scl type CVs, but such amplitude shows that the star has not reached a deep minimum of brightness as the ones observed in MV Lyr, TT Ari, and KR Aur (e.g. Leach & Hessman 1999). The data from ASAS-SN and CRTS was converted to V band, joined, and then sent to periodogram analysis. No significant intrinsic large-scale periodicity was found in this data set.

#### 3.1 Search for superhumps

Our first two observations of BG Tri in August 2020 showed light curves with large amplitude variations. The subsequent multi-band monitoring of the star reveals variations in brightness within four hours. The expected ellipsoidal variations would produce double orbital frequency modulation and the secondary shows no significant contribution to the total flux (Hernández et al. 2021). Another argument against this interpretation of the variations is that due to the low system inclination,  $i = 25(5)^\circ$ , the system is visible face-on, and these would be insufficient to modulate the light curves. Thus, the obvious 4-hour variations may be evidence for the existence of superhumps. To further study this, several long consequent observational runs were carried out at NAO Rozhen. The obtained data are presented in Figure 1. All data points were analysed using the Lomb-Scargle (Lomb 1976; Scargle 1982) and CLEAN algorithms (Roberts et al. 1987). A strictly periodic signal with  $P = 0.1516(2)$  days was detected in 2020 light curves. This period is slightly shorter than the orbital period of the system and represents a negative superhump. The next step was to analyse the available sky survey data. They were separated in seasons of visibility - BG Tri is visible in the sky

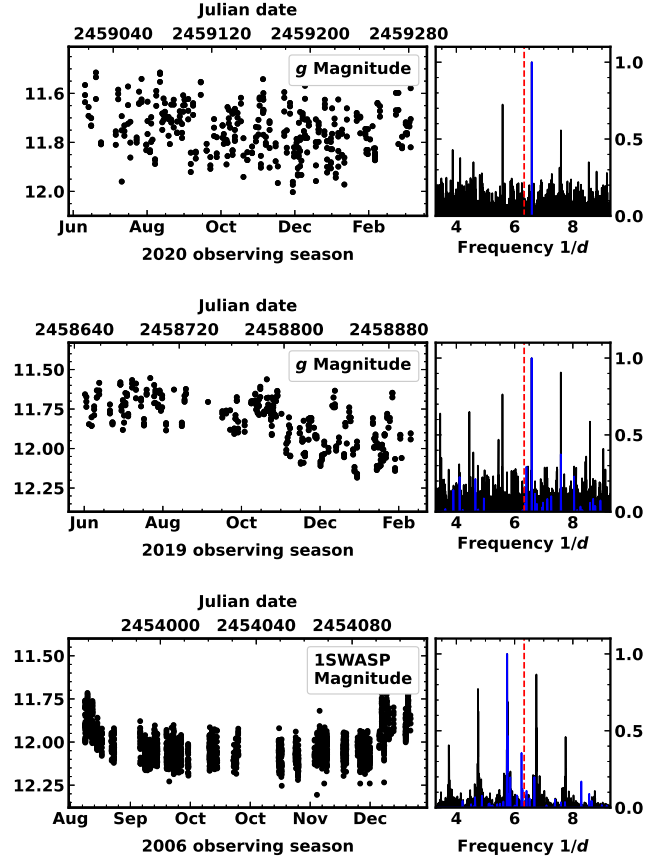


**Figure 3.** Normalised power spectra of the observing seasons containing significant periodic signals. Light curves and power spectra are shown on the right and left respectively. The top two rows contain data from ASAS-SN. The bottom row shows data from the WASP survey. The CLEAN periodograms are shown in blue and Lomb-Scargle in black. The red dashed vertical line is the orbital frequency of BG Tri.

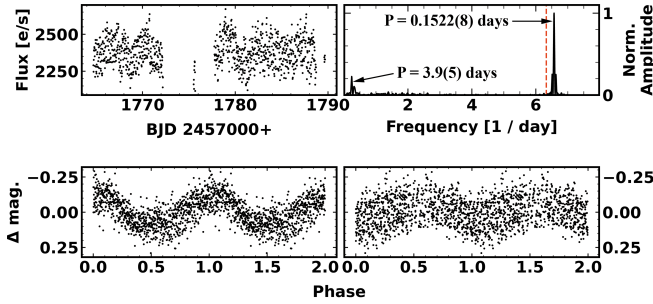
from June to February. The observing season is labeled by the year of the beginning of observations, even if some measurements were made in the first months of the next year. The seasons with enough data points were analysed with the same period search algorithms cited above. Strong periodic signals are found in seasons 2006, 2019 and 2020. The resulting power spectra are shown in Figure 3. Season 2006 is entirely made of photometry from the WASP sky survey, modulated with  $P = 0.1727(14)$  days - 9% longer than the orbital period - a positive superhump. The ASAS-SN photometric data from 2019 and 2020 are in g band. Both seasons contain a periodic variation with  $P = 0.1515(2)$  days, a negative superhump 5% shorter than  $P_{orb}$ . All measured periods and their uncertainties are shown in Table 2. We did not find significant evidence for the presence of superhumps during the observations in 2017 and 2018 of Hernández et al. (2021).

TESS observations provide continuous photometry of BG Tri from 07.10.2019 to 02.11.2019, with two gaps - one due to data transfer during perigee and one due to low-quality data. The periodogram analysis shown in Figure 4 reveals two significant periodicities:

- (i) Negative superhump with  $P = 0.1522(8)$  days. The superhump period from ASAS-SN data of the same season has a matching period within the uncertainty range.
- (ii) Superorbital variation with  $P = 3.94(53)$  days. This variation

**Table 2.** Significant periods from the power spectra.

| Data set               | Period [days] |
|------------------------|---------------|
| NAO Rozhen season 2020 | 0.1516(2)     |
| ASAS SN season 2020    | 0.1515(2)     |
| ASAS SN season 2019    | 0.1514(2)     |
| TESS sector 17 2019    | 0.1522(8)     |
| TESS sector 17 2019    | 3.94(53)      |
| WASP season 2006       | 0.1727(14)    |

**Figure 4.** Top: The extracted TESS light curve of BG Tri and its Lomb-Scargle power spectrum. The red vertical line represents the orbital frequency of the binary. Bottom: Data phased with  $P = 0.152$  days on the left and with  $P = 3.94$  days on the right.

is not present in ASAS-SN data, likely due to the limited amount of data and low time resolution.

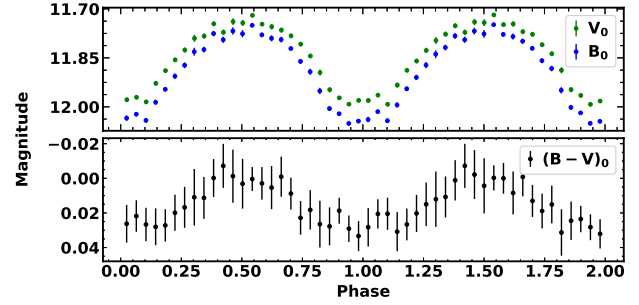
### 3.2 The negative superhumps of BG Tri

Negative superhumps are interpreted as a result of the gas stream sweeping across the face of a tilted disc. In a non-tilted disc, the disc overflow is the same on both sides, but in a slightly tilted disc, the overflow would be bigger on one side. If the disc is precessing, the overflow would then be modulated with the beat period of the disc precession and the orbital period of the binary, thus, creating the negative superhump. If this is the case, we would expect the precession period of the disc  $P_{prec}$  to be:

$$\frac{1}{P_{prec}} = \frac{1}{P_{-sh}} - \frac{1}{P_{orb}}. \quad (1)$$

Using the negative superhump period from TESS sector 17 ( $P_{-sh} = 0.1522(8)$  d) and the orbital period  $P_{orb} = 0.15845(10)$  d from Hernández et al. (2021), the expected value for  $P_{prec}$  is 3.8(5) days. The other major periodicity found in the TESS data is  $P = 3.94(53)$  days, co-existing with the negative superhump period. This we interpret as the precession period of the tilted accretion disc. The precession phase curve is on the bottom right panel of Figure 4. The simultaneous presence of negative superhumps and superorbital period in TESS the data is good evidence that both result from a tilted precessing disc.

Our multi-color observations show the full amplitudes of the negative superhump in the five bands to be  $-\Delta U = 0.30$  mag,  $\Delta B = 0.28$ ,  $\Delta V = 0.24$ ,  $\Delta R = 0.22$ , and  $\Delta I = 0.20$  mag. The  $B$  and  $V$  magnitudes of the used comparison stars are taken from Henden et al. (2015). To account for the interstellar extinction, we used  $E(B - V) = 0.03$  from Green et al. (2015). The  $(B - V)_0$  color of BG Tri phased with the negative superhump period is shown in Figure 5. This  $(B - V)_0$  phase curve is created using phase-binned photometry in the two bands

**Figure 5.** The upper panel shows the binned phase curve (25 bins) of the negative superhump in the dereddened  $B$  with blue dots and in dereddened  $V$  with green dots. The error bars represent the standard error of the data in each bin. The bottom panel is the resulting  $(B - V)_0$  color for each bin.

from multiple nights with an equal cadence. Its bluest peak corresponds to the maximum brightness of the superhump. This result is similar to the color index behaviour of ER UMa (Imada et al. 2018) and differs from the case of MASTER J1727, where the bluest peak coincides with the ascending branch of the phase curve (Pavlenko et al. 2019).

### 3.3 Disc tilt

The tilt angle of the disc is a function of the phase curve amplitude of the nodal precession variability. As the disc precesses, its projected area increases and decreases periodically, thus creating the superorbital variability. Most systems that exhibit this type of disc precession have tilts of a few degrees (e.g., Kimura et al. 2020; Kimura & Osaki 2021). BG Tri's disc tilt can be estimated using the amplitude-tilt relation derived in Smak (2009):

$$\delta = A * 52.770 \frac{(1 - u + u \cos i) \cos i}{(1 - u + 2u \cos i) \sin i}, \quad (2)$$

where  $u$  is the limb darkening coefficient,  $i$  is the system inclination, and  $A$  is the semi-amplitude in magnitudes. Using  $u = 0.6$ ,  $i = 25^\circ$  from Hernández et al. (2021), and  $A = 0.05$  mag, measured by fitting a sine curve to the phase plot of the precession variability (bottom right panel on Fig. 4), a value of  $\delta \approx 3^\circ$  is obtained. This is the typical value for disc tilts in CVs that display negative superhumps (Smak 2009).

### 3.4 The positive superhumps of BG Tri

Positive superhumps are interpreted as a result of the apsidal precession of an elliptical accretion disc, driven by a 3:1 resonance (Whitehurst 1988; Hirose & Osaki 1990; Lubow 1991). The resonance induces tidal deformations in the disc, which manifest as brightness variations due to periodic heating. Positive superhumps in BG Tri are discovered in archival WASP data from 2006. This is the only dataset with detected positive superhumps. Phase curve of the data folded with the most significant period -  $P_{+sh} = 0.1727(14)$  days is shown in Figure 6.

### 3.5 System parameters

Superhumps can be used to reveal the mass ratio  $q = M_2/M_1$  using the excess/deficit of the positive/negative superhump:

$$\varepsilon_{+/-} = \frac{P_{+/-sh} - P_{orb}}{P_{orb}}. \quad (3)$$



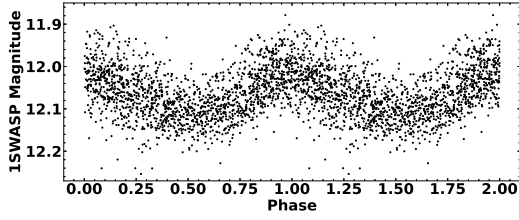


**Figure 6.** Phase curve of the positive superhump of BG Tri - the WASP data from 2006 folded with  $P = 0.1727$  days.

For BG Tri the values of  $\varepsilon_-$  and  $\varepsilon_+$  are 0.044(1) and 0.090(9) respectively. The ratio  $\varepsilon_+/\varepsilon_- = 2.0(2)$  is in agreement with the value of  $\sim 2$  for systems that show both types of superhumps (Patterson et al. 1997; Wood et al. 2009). The excess and deficit are shown to correlate with  $q$ . In Wood et al. (2009), relation between  $\varepsilon_-$  and  $q$  is derived from particle simulations:

$$q = -0.192|\varepsilon_-|^{1/2} + 10.37|\varepsilon_-| - 99.83|\varepsilon_-|^{3/2} + 451.1|\varepsilon_-|^2. \quad (4)$$

This relation gives a value of  $q = 0.37(2)$ . For the positive superhump, we used the experimentally derived relation  $q(\varepsilon_+)$  in Kato (2022), assuming that the measured  $\varepsilon_+$  is a stage B superhump excess. This gives us again  $q = 0.40(5)$ . The uncertainty estimation for  $q$  is done using only errors from the periodogram analysis. These relations provide values for  $q$  that are in agreement with Hernández et al. (2021), where the WD mass was assumed to be  $0.8M_\odot$  since this is the average WD mass for binaries above the period gap (Zorotovic et al. 2011). With the average value of the system’s mass ratio  $q = 0.39(3)$  (averaged by the positive and the negative superhump estimations) and mass of the secondary  $0.35M_\odot$ <sup>1</sup> of the secondary  $R_2 = 0.40R_\odot$  by Eq. (2.100) in Warner (2003), from the mass-period relationship in Warner (2003), we calculate the mass of the white dwarf  $M_1 = 0.91(7)M_\odot$ . Using these parameters, the binary separation is  $a = 1.33(2)R_\odot$  and the truncation radius of the accretion disc<sup>2</sup> is  $r_d = 0.58(2)R_\odot$ . We note that the primary Roche lobe radius derived by Eggleton (1983) is  $r_L = 0.62(1)R_\odot$ , which means that the accretion disc in BG Tri fills about 93% of the primary Roche lobe. This is in good agreement with the maximum size of the discs in non-magnetic nova-like CVs (Harrop-Allin & Warner 1996).

### 3.6 Quasi-periodic oscillations and flickering

Fast variations in brightness in timescales of seconds to minutes are typical for cataclysmic variables. Their amplitudes are the largest in  $U$  band and can vary from a few hundredths to a few tenths of a magnitude. They are erratic and highly unstable and can change significantly from night to night. QPOs are generally observed in systems with high transfer rates and are believed to be originating from the inner accretion disc. To study these phenomena and compare BG Tri with other similar systems, the approach presented by Bruch (2021) was followed. A Savitzky-Golay filter (Savitzky & Golay 1964) with a cutoff time scale  $\Delta t = 60$  min and a 4<sup>th</sup> degree smoothing polynomial was applied and subtracted from all light curves in the  $V$  band longer than 2 hours. Then, the weighted wavelet Z-transform (WWZ) method by Foster (1996) was used to detect and display the evolution

of the QPOs in BG Tri. A sample of the acquired two-dimensional spectra are shown in Figure 8. Typical QPO periods for BG Tri are in the range of 5–25 min, similar to other CVs - e.g., TT Ari and V729 Sgr (Bruch 2019; Sun et al. 2022). A summary of the WWZ analysis for all selected nights is shown in Table 4. Distribution of the detected QPO periods is shown in Figure 9. Overlapping of multiple oscillations with different periods is also present in some of the data. Most of them remain coherent for 3 to more than 10 cycles. Their period and stability vary from night to night - there were no QPOs lasting for more than 3 cycles seen on 14 Oct 2020, but the 14 minute QPO seen in the light curve from 25 Sep 2020 lasts for 11 cycles. Figure 7 shows this behaviour with fitted sines to the QPOs in the data. Sudden changes in period similar to the ones observed in TT Ari by Kraicheva et al. (1999) are also displayed by BG Tri.

If we suppose that the QPOs in BG Tri occur in dynamical time scale ( $t_{dyn}$ ) related to the Keplerian rotation around the primary, we could determine the possible locations of the observed variations. For  $t_{dyn}$  we use the scaled relation in Sokolowski (2003):

$$t_{dyn} = 4s \left( \frac{r}{10^9 cm} \right)^{3/2} \left( \frac{M_{WD}}{0.6M_\odot} \right)^{-1/2}. \quad (5)$$

Here  $r$  is the distance from the primary (white dwarf) and  $M_{WD}$  is the mass of the primary. Replacing the values of  $M_{WD}$  and  $r_d$  from Section 3.5 into Eq. 5 and taking into account their uncertainties, for  $t_{dyn}$  we obtain:  $t_{dyn} = 14(1)$  min. This result makes it possible to assume that the observed QPOs in the range of 12 – 14 minutes are connected with the outer disc rim, or the overflow of matter from the back side of the disc in BG Tri proposed by Hernández et al. (2021). The full range of the detected QPOs (5 – 25min.) corresponds to the range of distances  $R = 0.28(1) - 0.82(3)R_\odot$  from the white dwarf. The origin of the fastest ones may be related to the formation of ‘clumps’ or turbulent eddies in the process of transporting matter through the disc.

In his study of flickering in CVs, Bruch (2021) defines the  $A_{60}$  amplitude of flickering. After applying the Savitzky-Golay filter as discussed above, the magnitude distribution of each light curve is fitted with a normal distribution, and its FWHM is the  $A_{60}$  amplitude. All light curve data were binned to the same cadence before  $A_{60}$  amplitudes were measured. The contribution of the secondary is insignificant (Hernández et al. 2021) and no correction was applied. A minimum of 25 hours of high cadence photometric data in all five bands were acquired during season 2020 on site observations. BG Tri was in a negative superhump regime on all of these nights. Our data from this season shows that the  $A_{60}$  amplitudes are highest in  $U$  band - 0.13 mag. The amplitudes in the other filters are similar but decrease to the red bands with  $\Delta R$  and  $\Delta I$  being 0.09 and 0.08 mag, respectively. In the following season 2021, our observations consist of minimum 8 hours of high cadence data in the five bands. During this season the negative superhump is not present in the light curves, and the  $A_{60}$  amplitudes in all bands are half as low those measured in 2020. The amplitudes during season 2020 are similar to other VY Scl sub-type stars and during season 2021 resemble those of UX UMa sub-type (Bruch 2021). The measured amplitudes from both seasons are shown in Table 3.

## 4 CONCLUSIONS

In this work, we present the first photometric study of the bright cataclysmic variable BG Triangulum. Our light curve analysis yields the following results:

<sup>1</sup> The same result can be obtained with the mass-radius relation in Demircan & Kahraman (1991), using the size

<sup>2</sup> Given by Eq. (2.61)  $r_d = 0.60a/(1+q)$  in Warner (2003).

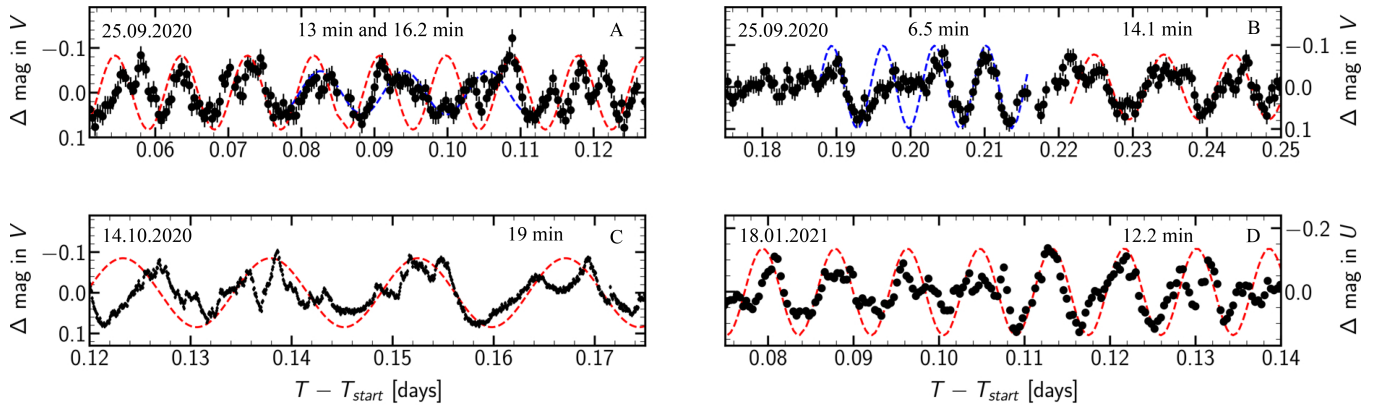


**Figure 7.** Sinusoidal fits using periods from the spectral analysis of some of the light curves.

**Table 3.** Average values of the flickering amplitude  $A_{60}$  measured in the  $UBVRI$  bands for BG Tri. The numbers in brackets are the standard deviation of  $A_{60}$  derived from different light curves and the number of light curves upon which the average values are based.

| Data set    | $A_{60}(U)$     | $A_{60}(B)$       | $A_{60}(V)$     | $A_{60}(R)$       | $A_{60}(I)$       |
|-------------|-----------------|-------------------|-----------------|-------------------|-------------------|
| Season 2020 | 0.13 (0.02) (7) | 0.10 (0.02) (8)   | 0.09 (0.02) (8) | 0.09 (0.01) (6)   | 0.08 (0.01) (6)   |
| Season 2021 | 0.06 (0.01) (3) | 0.041 (0.004) (3) | 0.04 (0.01) (6) | 0.052 (0.008) (3) | 0.050 (0.008) (3) |

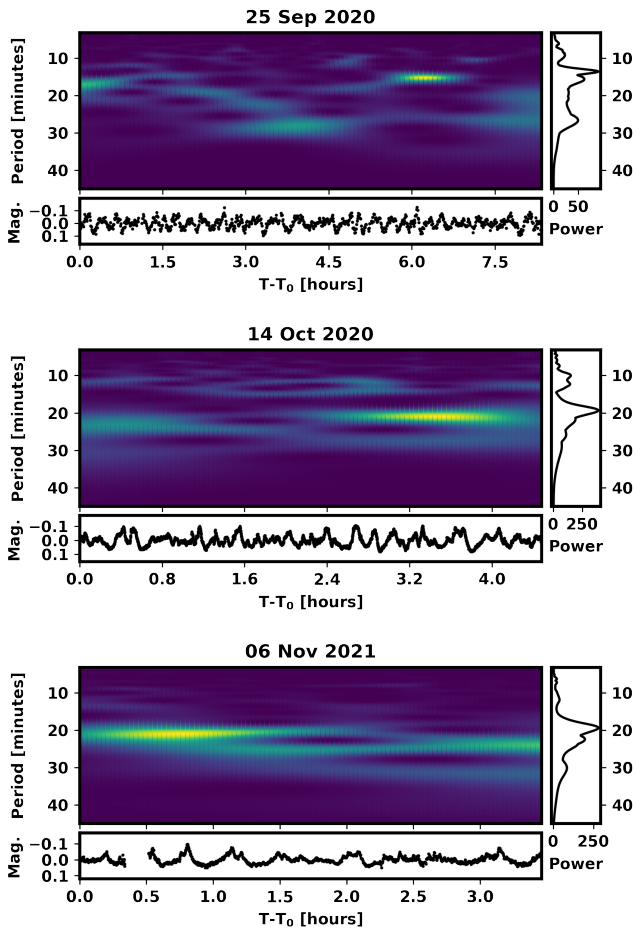


**Figure 8.** Two-dimensional power spectra of three nights using WWZ.

**Table 4.** Summary of the quasi-periodic oscillations detected in BG Tri.

| Date       | P [minutes] | Date       | P [minutes] |
|------------|-------------|------------|-------------|
| 2020/09/22 | 17.3(±7)    | 2021/01/18 | 6.5 (±1.5)  |
|            | 15.8(±7)    |            | 12 (±1)     |
|            | 14.5(±7)    |            | 9.5 (±1.1)  |
|            | 12.8(±9)    |            | 14.3(±1.3)  |
|            | 10.7(±2)    |            | 4.4 (±0.6)  |
| 2020/09/23 | 18 (±1)     | 2021/10/30 | 20.4(±4.6)  |
|            | 16 (±1)     |            | 13.3(±1.1)  |
|            | 23.5(±2.5)  |            | 3.7 (±0.6)  |
| 2020/09/24 | 21.5(±3.5)  | 2021/11/06 | 19.4(±1.3)  |
|            | 10.1(±1.6)  |            | 22.5(±1.2)  |
| 2020/09/25 | 6.8 (±1.3)  | 2021/11/07 | 11.9(±2.2)  |
|            | 13.5(±0.9)  |            | 7.2 (±0.7)  |
|            | 15.6(±1.6)  |            | 6.2 (±0.6)  |
|            | 26.6(±2.6)  |            | 5.2 (±0.3)  |
|            | 19.2(±1.4)  |            | 16.2(±2.7)  |
| 2020/10/14 | 6.1 (±0.8)  | 2021/11/08 | 23.9(±3.6)  |
|            | 19.3(±3.4)  |            | 10.2(±2)    |
|            | 10 (±1)     |            | 18.4(±1.1)  |
|            | 12 (±1)     |            | 5.1 (±0.9)  |

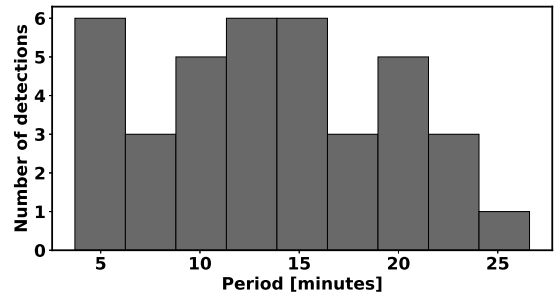


**Figure 9.** Distribution of the QPO periods found with the WWZ method.

- Positive superhumps are discovered in data from the WASP sky survey. They appear only in 2006 data with period  $P_{+sh} = 0.1727(14)$  days. This gives a value of the excess  $\varepsilon_+ = 0.090(9)$ . Using this excess, the mass ratio  $q$  is estimated to be  $q_+ = 0.40(5)$ .

- Negative superhumps are discovered in our observations from season 2020 and in data from the ASAS-SN sky survey. They appear in season 2019 after an year-long low VY-Scl state and disappear in season 2021. During these two years, we did not find a significant change in the superhump period -  $P_{-sh} = 0.1515(2)$  days. This gives a superhump deficit  $\varepsilon_- = 0.044(1)$  and  $q_- = 0.37(2)$ .

- A superorbital variation is present in photometry from the TESS mission. It has a period of 3.94(53) days and an amplitude of 0.05 mag. Using this amplitude, we estimate the tilt of the disc of BG Tri to be  $\approx 3^\circ$ .

- Our study of the quasi-periodic oscillations of BG Tri shows that the most common quasi-periods are in the range of 5–25 min. During our observations in season 2020, BG Tri was in a negative superhump regime, and we find the amplitude to be the highest in  $U$  band ( $\Delta U = 0.13$  mag) and decrease to the red bands ( $\Delta I = 0.08$  mag). In season 2021 when the superhump is gone, the amplitudes of the QPOs are systematically lower ( $\Delta U = 0.06$  mag, and in  $I$  band is 0.05 mag).

BG Tri is a good candidate for the study of CV accretion discs. Its relative brightness in high state allows it to be a great target even for amateur astronomers. The system should be monitored in the future to study the nature of superhump appearance and disappearance.

## ACKNOWLEDGEMENTS

We are grateful to the organizers of the "Beli Brezi" summer school of astronomy and the team working with the 25 cm Newton telescope. We also wish to thank the team of Andromeda Observatory for the data they kindly provided us. This study is using publicly available data from the TESS mission, ASAS-SN, WASP, CRTS, and NSVS. We express our gratitude to the teams of these sky surveys for making their data public.

This study is supported by the grant KII-6-H28/2 - Binary stars with compact object (Bulgarian national science fund).

We appreciate the anonymous reviewer's valuable comments and suggestions, which helped us to improve the quality of the manuscript.

## DATA AVAILABILITY

The non-public data underlying this article will be shared on reasonable request to the corresponding authors.

## REFERENCES

Astropy Collaboration et al., 2013, *A&A*, **558**, A33  
 Astropy Collaboration et al., 2018, *AJ*, **156**, 123  
 Belova A. I., Suleimanov V. F., Bikmaev I. F., Khamitov I. M., Zhukov G. V., Senio D. S., Belov I. Y., Sakhibullin N. A., 2013, *Astronomy Letters*, **39**, 111  
 Brasseur C. E., Phillip C., et al. 2019, *Astrocut: Tools for creating cutouts of TESS images* (ascl:1905.007)  
 Bruch A., 2019, *MNRAS*, **489**, 2961  
 Bruch A., 2021, *MNRAS*, **503**, 953  
 Butters O. W., et al., 2010, *A&A*, **520**, L10  
 Castro Segura N., et al., 2021, *MNRAS*, **501**, 1951  
 Demircan O., Kahraman G., 1991, *Ap&SS*, **181**, 313

Drake A. J., et al., 2009, *ApJ*, **696**, 870  
 Eggleton P. P., 1983, *ApJ*, **268**, 368  
 Foster G., 1996, *AJ*, **112**, 1709  
 Ginsburg A., et al., 2019, *AJ*, **157**, 98  
 Green G. M., et al., 2015, *ApJ*, **810**, 25  
 Haakonsen C. B., Rutledge R. E., 2009, *ApJS*, **184**, 138  
 Harrop-Allin M. K., Warner B., 1996, *MNRAS*, **279**, 219  
 Hellier C., 2001, *Cataclysmic Variable Stars: How and Why They Vary*. Springer-Praxis, Chichester, UK  
 Henden A. A., Levine S., Terrell D., Welch D. L., 2015, in *American Astronomical Society Meeting Abstracts #225*. p. 336.16  
 Hernández M. S., Tovmassian G., Zharikov e. a., 2021, *MNRAS*, **503**, 1431  
 Hirose M., Osaki Y., 1990, *PASJ*, **42**, 135  
 Ikiewicz K., et al., 2021, *MNRAS*, **503**, 4050  
 Imada A., Yanagisawa K., Kawai N., 2018, *PASJ*, **70**, L4  
 Jockers K., et al., 2000, *Kinematika i Fizika Nebesnykh Tel Suppl.*, **3**, 13  
 Kato 2018, [vsnet-chat 8117] VY Scl-type object currently in faint state  
 Kato T., 2022, arXiv e-prints, p. arXiv:2201.02945  
 Kato T., et al., 2009, *PASJ*, **61**, S395  
 Kato T., et al., 2017, *PASJ*, **69**, 75  
 Khruslov A. V., 2008, *Peremennye Zvezdy Prilozhenie*, **8**, 4  
 Kimura M., Osaki Y., 2021, *PASJ*, **73**, 1225  
 Kimura M., Osaki Y., Kato T., 2020, *PASJ*, **72**, 94  
 Kochanek C. S., et al., 2017, *PASP*, **129**, 104502  
 Kraicheva Z., Stanishev V., Genkov V., Iliev L., 1999, *A&A*, **351**, 607  
 Leach R., Hessman e., 1999, *MNRAS*, **305**, 225  
 Lightkurve Collaboration et al., 2018, *Lightkurve: Kepler and TESS time series analysis in Python*, *Astrophysics Source Code Library* (ascl:1812.013)  
 Lomb N. R., 1976, *Ap&SS*, **39**, 447  
 Lubow S. H., 1991, *ApJ*, **381**, 259  
 Makarov V. V., 2017, *Rev. Mex. Astron. Astrofis.*, **53**, 439  
 Montgomery M. M., 2009, *MNRAS*, **394**, 1897  
 Patterson J., Kemp J., Saad J., Skillman D. R., Harvey D., Fried R., Thorstensen J. R., Ashley R., 1997, *PASP*, **109**, 468  
 Pavlenko E., et al., 2019, in *Tovmassian G. H., Gansicke B. T., eds, Compact White Dwarf Binaries*. p. 39  
 Pavlenko E. P., Sosnovskij A. A., Antoniuik K. A., Lyumanov E. R., Pit N. V., Antoniuik O. I., 2020, *Astrophysics*,  
 Rawat N., Pandey J. C., Joshi A., Yadava U., 2022, *MNRAS*, **512**, 6054  
 Ricker G. R., et al., 2015, *Journal of Astronomical Telescopes, Instruments, and Systems*, **1**, 014003  
 Ritter H., Kolb U., 2005, *VizieR Online Data Catalog*, p. V/113D  
 Roberts D. H., Lehar J., Dreher J. W., 1987, *AJ*, **93**, 968  
 Savitzky A., Golay M. J. E., 1964, *Analytical Chemistry*, **36**, 1627  
 Scargle J. D., 1982, *ApJ*, **263**, 835  
 Shappee B. J., et al., 2014, *ApJ*, **788**, 48  
 Smak J., 2009, *Acta Astron.*, **59**, 419  
 Sokoloski J. L., 2003, in *Corradi R. L. M., Mikolajewska J., Mahoney T. J., eds, Astronomical Society of the Pacific Conference Series Vol. 303, Symbiotic Stars Probing Stellar Evolution*. p. 202 (arXiv:astro-ph/0209101)  
 Stefanov S. Y., 2021, *Bulgarian Astron. J.*, **36**, arXiv:2106.03568  
 Sun Q.-B., et al., 2022, *New Astron.*, **93**, 101751  
 Warner B., 2003, *Cataclysmic Variable Stars*, doi:10.1017/CBO9780511586491.  
 Whitehurst R., 1988, *MNRAS*, **232**, 35  
 Wood M. A., Thomas D. M., Simpson J. C., 2009, *MNRAS*, **398**, 2110  
 Woźniak P. R., et al., 2004, *AJ*, **127**, 2436  
 Zorotovic M., Schreiber M. R., Gänsicke B. T., 2011, *A&A*, **536**, A42

This paper has been typeset from a  $\text{\TeX}/\text{\LaTeX}$  file prepared by the author.